

1

2 **Interferon Resistance of Emerging SARS-CoV-2 Variants**

3

4 Kejun Guo¹, Bradley S. Barrett¹, Kaylee L. Mickens^{1,2}, Ezster K. Vladar³,
5 James H. Morrison¹, Kim J. Hasenkrug⁴, Eric M. Poeschla¹, and Mario L. Santiago^{1,2*}

6

7 *¹Division of Infectious Diseases, Department of Medicine,*

8 *University of Colorado Anschutz Medical Campus, Aurora, CO, USA 80045*

9

10 *²Department of Immunology and Microbiology,*

11 *University of Colorado Anschutz Medical Campus, Aurora, CO, USA 80045*

12

13 *³Division of Pulmonary Sciences and Critical Medicine, Department of Medicine,*

14 *University of Colorado Anschutz Medical Campus, Aurora, CO, USA 80045*

15

16 *⁴Rocky Mountain Laboratories, National Institutes of Allergy and Infectious Diseases,*

17 *National Institutes of Health, Hamilton, MT 59840*

18

19

20 *To whom correspondence should be addressed: mario.santiago@ucdenver.edu

21

22

23 **Abstract**

24 The emergence of SARS-CoV-2 variants with enhanced transmissibility, pathogenesis and
25 resistance to vaccines presents urgent challenges for curbing the COVID-19 pandemic. While
26 Spike mutations that enhance virus infectivity or neutralizing antibody evasion may drive the
27 emergence of these novel variants, studies documenting a critical role for interferon responses in
28 the early control of SARS-CoV-2 infection, combined with the presence of viral genes that limit
29 these responses, suggest that interferons may also influence SARS-CoV-2 evolution. Here, we
30 compared the potency of 17 different human interferons against multiple viral lineages sampled
31 during the course of the global outbreak, including ancestral and four major variants of concern.
32 Our data reveal increased interferon resistance in emerging SARS-CoV-2 variants, suggesting
33 that evasion of innate immunity may be a significant, ongoing driving force for SARS-CoV-2
34 evolution. These findings have implications for the increased lethality of emerging variants and
35 highlight the interferon subtypes that may be most successful in the treatment of early infections.

36

37 **Author Summary**

38 In less than 2 years since its spillover into humans, SARS-CoV-2 has infected over 220 million
39 people, causing over 4.5 million COVID-19 deaths. High infection rates provided substantial
40 opportunities for the virus to evolve, as variants with enhanced transmissibility, pathogenesis,
41 and resistance to vaccine-elicited neutralizing antibodies have emerged. While much focus has
42 centered on the Spike protein which the virus uses to infect target cells, mutations were also
43 found in other viral proteins that might inhibit innate immune responses. Specifically, viruses
44 encounter a potent innate immune response mediated by the interferons, two of which, IFN α 2
45 and IFN β , are being repurposed for COVID-19 treatment. Here, we compared the potency of

46 human interferons against ancestral and emerging variants of SARS-CoV-2. Our data revealed
47 increased interferon resistance in emerging SARS-CoV-2 strains that included the alpha, beta,
48 gamma and delta variants of concern, suggesting a significant, but underappreciated role for
49 innate immunity in driving the next phase of the COVID-19 pandemic.

50

51 Results

52 The human genome encodes a diverse array of antiviral interferons (IFNs). These include the
53 type I IFNs (IFN-Is) such as the 12 IFN α subtypes, IFN β and IFN ω that signal through
54 ubiquitous IFNAR receptor, and the type III IFNs (IFN-IIIIs) such as IFN λ 1, IFN λ 2 and IFN λ 3
55 that signal through the more restricted IFN λ R receptor that is present in lung epithelial cells [1].
56 IFN diversity may be driven by an evolutionary arms-race in which viral pathogens and hosts
57 reciprocally evolve countermeasures [2]. For instance, the IFN α subtypes exhibit >78% amino
58 acid sequence identity, but IFN α 14, IFN α 8 and IFN α 6 most potently inhibited HIV-1 *in vitro*
59 and *in vivo* [3-5], whereas IFN α 5 most potently inhibited influenza H3N2 in lung explant
60 cultures [6]. Even though SARS-CoV-2 was sensitive to IFN α 2, IFN β , and IFN λ [7-9], and
61 clinical trials of IFN α 2 and IFN β demonstrated therapeutic promise for COVID-19 [10-12], a
62 direct comparison of multiple IFN-Is and IFN-IIIIs against diverse SARS-CoV-2 variants of
63 concern has not yet been done.

64

65 The current study was initially undertaken to determine which IFNs would best inhibit SARS-
66 CoV-2. These first set of experiments were performed between December 2020 and March 2021,
67 and we selected 5 isolates from prominent lineages [13] during this phase of the pandemic (Fig
68 1, S1 Table). USA-WA1/2020 is the standard strain utilized in many *in vitro* and *in vivo* studies
69 of SARS-CoV-2 and belongs to lineage A [13]. It was isolated from the first COVID-19 patient
70 in the US, who had a direct epidemiologic link to Wuhan, China, where the virus was first
71 detected [14]. By contrast, subsequent infection waves from Asia to Europe [15] were associated
72 with the emergence of the D614G mutation [16]. Lineage B strains with G614 spread globally
73 and displaced ancestral viruses with striking speed, likely due to increased transmissibility [17],

74 18]. These strains accumulated additional mutations in Italy as lineage B.1 which then
75 precipitated a severe outbreak in New York City [19]. Later in the United Kingdom (U.K.),
76 lineage B.1.1.7 acquired an N501Y mutation associated with enhanced transmissibility [13].
77 Lineage B.1.351, first reported in South Africa, additionally acquired an additional E484K
78 mutation associated with resistance to neutralizing antibodies [20, 21]. Both B.1.1.7 and B.1.351
79 were reported in multiple countries and in some cases have become dominant for extended
80 periods [22]. We obtained representative SARS-CoV-2 isolates of the B, B.1, B.1.1.7 and
81 B.1.351 lineages (S1 Table). Each stock was sourced from beiresources.org and amplified once
82 in a human alveolar type II epithelial cell line (A549) that we have stably transduced with the
83 receptor ACE2 (A549-ACE2) (S1A Fig).

84

85 A549-ACE2 cells were pre-incubated with 17 recombinant IFNs (PBL Assay Science) overnight
86 in parallel and in triplicate, then infected with a non-saturating virus dose for 2 h (S1B Fig). We
87 normalized the IFNs based on molar concentrations similarly to our previous work with HIV-1
88 [3, 23]. To enable high-throughput evaluation of the antiviral activities of the numerous IFNs
89 against the multiple live SARS-CoV-2 isolates, we used a quantitative PCR (qPCR) assay to
90 determine amounts of virus produced 24 hours after infection (Fig 2A). Initial dose-tiltrations
91 showed that a 2 pM concentration fell within the dynamic range of activity and maximally
92 distinguished the antiviral activities of IFNs with widely divergent potencies, i.e., IFN β and
93 IFN λ 1 (S1C Fig). Of note, the IFN β and IFN λ 1 doses used did not significantly affect cell
94 viability (S1D Fig). Thus, 2 pM doses were used for additional antiviral activity testing. We also
95 evaluated the qPCR assay against a VeroE6 plaque assay using triplicate serial dilutions of a
96 SARS-CoV-2 isolate (B.1.351). Virus titers obtained using these two assays were strongly

97 correlated (S2A Fig). However, the VeroE6 plaque assay had ~2-log lower dynamic range; we
98 estimate that 1 plaque forming unit corresponds to ~900 SARS-CoV-2 N1 copies (S2A Fig).
99 Virus copy numbers also correlated with the numbers of primary airway epithelial cells infected
100 with different SARS-CoV-2 variants as quantified by immunofluorescence (S2B Fig). Thus, we
101 employed the qPCR assay to robustly distinguish the antiviral activity of the different
102 interferons.

103

104 In the absence of IFN, all 5 isolates reached titers of $\sim 10^4$ - 10^6 copies per 5 μ l input of RNA
105 extract (Fig 2). Using absolute copy numbers (Fig 2) or values normalized to mock as 100% (S2
106 Fig), the 17 IFNs showed a range of antiviral activities against SARS-CoV-2. The 3 IFN λ
107 subtypes exhibited none to very weak (<2-fold) antiviral activities compared to most IFN-Is (Fig
108 2 and S3 Fig, blue bars). This was despite the fact that the assay showed a robust dynamic range,
109 with some IFNs inhibiting USA-WA1/2020 >2500-fold to below detectable levels (Fig 2A). IFN
110 potencies against the 5 isolates correlated with each other (S4 Fig), and a similar rank-order of
111 IFN antiviral potency was observed for G614+ isolates (Fig 2B, S3 Fig). Overall, IFN α 8, IFN β
112 and IFN ω were the most potent, followed by IFN α 5, IFN α 17 and IFN α 14 (Fig 2C); the type III
113 (λ) IFNs were least potent.

114

115 The molecular basis for the diverse antiviral effects of the highly related IFN α subtypes has been
116 an active area of investigation, particularly with regard to the relative contributions of
117 quantitative (signaling) versus qualitative (differential gene regulation) mechanisms [2-5]. We
118 reported that inhibition of HIV-1 by the IFN α subtypes correlated with IFNAR signaling
119 capacity and binding affinity to the IFNAR2 subunit [3, 23]. IFNAR signaling capacity, as

120 measured in an IFN-sensitive reporter cell line (iLite cells; Euro Diagnostics), correlated with the
121 antiviral potencies of the IFN α subtypes against SARS-CoV-2 lineages A and B, but not B.1,
122 B.1.351 or B.1.1.7 (Fig 3A). IFNAR binding affinities as measured by surface plasmon
123 resonance by the Schreiber group [24] did not correlate with IFN α subtype inhibition of SARS-
124 CoV-2 (Fig 3B). As the recombinant IFNs used in this study was from the same source as that of
125 the prior HIV-1 study [3, 23], we also determined if the IFNs that potently inhibit HIV-1 also
126 function similarly against SARS-CoV-2. Notably, the correlations between SARS-CoV-2 and
127 HIV-1 inhibition [3] were weak at best (Fig 3C). These findings suggested that IFN-mediated
128 control of SARS-CoV-2 isolates may be qualitatively distinct from that of HIV-1.

129

130 We generated a heat-map to visualize the antiviral potency of diverse IFNs against the 5 isolates
131 and observed marked differences in IFN sensitivities (Fig 4A). Pairwise analysis of antiviral
132 potencies between isolates collected early (January 2020) and later (March-December 2020)
133 during the pandemic were performed against the 14 IFN-Is (IFN-III data were not included due
134 to low antiviral activity, Fig. 2). The overall IFN-I sensitivity of USA-WA1/2020 and
135 Germany/BavPat1/2020 isolates were not significantly different from each other (Fig 4B). In
136 contrast, relative to Germany/BavPat1/2020, we observed 17 to 122-fold IFN-I resistance of the
137 emerging SARS-CoV-2 variants (Fig 4C), with the B.1.1.7 strain exhibiting the highest IFN-I
138 resistance (this can also be seen in Fig. 3). The level of interferon resistance was especially
139 striking when compared to the early pandemic USA-WA1/2020 strain, where emerging SARS-
140 CoV-2 variants exhibited 25 to 322-fold higher IFN-I resistance (Fig 4D).

141

142 The experiments to this point allowed for the simultaneous analysis of 17 IFNs against multiple
143 SARS-CoV-2 isolates, but did not provide information on how different IFN-I doses affect virus
144 replication. It also remained unclear if the emerging variants were resistant to IFN-IIIs. We
145 therefore titrated a potent (IFN β ; 0.002 to 200 pM) and a weak (IFN λ 1; 0.02 to 2000 pM)
146 interferon against the lineage A, B, B.1, B.1.1.7 and B.1.351 viruses (Fig 5 and S5 Fig). Of note,
147 as the pandemic progressed in the past year, new variants of concern (VOCs) became dominant
148 in several countries; the WHO implemented a simplified Greek letter nomenclature for these
149 VOCs. We therefore included 3 additional VOCs, which were also obtained from the BEI
150 repository: (1) a second B.1.1.7 (alpha) isolate, England/204820464/2020; (2) an isolate from
151 lineage P.1 (gamma), which branched off from lineage B.1.1.28; and (3) an isolate from lineage
152 B.1.617.2 (delta) (S1 Table). Lineage P.1 was first described in an outbreak of SARS-CoV-2 in
153 Manaus, Brazil, which occurred in a population with high levels of prior infection. P.1
154 independently acquired the E484K mutation [25, 26] (Fig 1A, S1 Table). The delta strain was
155 first reported in India in early 2021 [27, 28], and as of July 2021, has become the dominant
156 variant worldwide, including the USA [29]. The delta strain was particularly concerning as it was
157 frequently observed in breakthrough infections among fully-vaccinated individuals [30, 31].

158

159 The lineage A and B isolates were similarly inhibited by IFN β and IFN λ 1 (S5A Fig). Comparing
160 B to B.1, the 50% inhibitory concentration (IC₅₀) of the B.1 isolate was 2.6 and 5.5-fold higher
161 IC₅₀ for IFN λ 1 and IFN β , respectively (S5B Fig). Comparing B to B.1.1.7, the B.1.1.7 variants
162 IC₅₀s were 4.3 to 8.3-fold higher for IFN β and 3.0 to 3.5 higher for IFN λ 1 (Fig 5A).
163 Interestingly, maximum inhibition was not achieved with either IFN β or IFN λ 1 against the
164 B.1.1.7 variant, plateauing at 15 to 20-fold higher levels than the ancestral lineage B isolate (Fig.

165 5A), which was in sharp contrast to the lineage B.1 isolate (S5B Fig). In a separate experiment,
166 the B.1.351 variant was also more resistant to IFN β (43-fold) and IFN λ 1 (26-fold) compared to
167 the lineage B isolate (Fig 5B). Here, however, maximum inhibition was achieved with IFN β . The
168 P.1 variant also exhibited higher resistance to IFN β (1.9-fold) and IFN λ 1 (4.4-fold), and the
169 plateau concentration for antiviral activity was >10-fold higher for IFN β than for the lineage B
170 isolate (Fig. 5C). Consistent with the findings with the other VOCs, the B.1.617.2 (delta) variant
171 was also more resistant to IFN β (6.7-fold) (Fig. 5D). Although similar IC50s were obtained with
172 IFN λ 1, the B.1.617.2 isolate had higher residual replication at the highest doses than the
173 ancestral lineage B isolate (Fig. 5D).

174

175 Two months after our initial preprint [32], Thorne *et al* posted data that in Calu-3 cells, a B.1.1.7
176 isolate, was more resistant to IFN β than a ‘first wave’ lineage B isolate [33]. We found that
177 lineage A and B isolates replicated poorly in Calu-3 cells, making these cells unsuitable for IFN
178 resistance comparisons between ancestral versus emerging variants (S6A Fig). This was in sharp
179 contrast to A549-ACE2 cells, where we observed high levels of virus production (>10⁵ copies)
180 of all strains studied (S1B Fig). Notably, comparable titers were obtained between the B.1 and
181 B.1.1.7 isolates in Calu-3 cells (S6A Fig). In these cells, the B.1.1.7 isolate was 50-fold more
182 resistant to IFN λ 1 than the B.1 isolate (S6B Fig). We also demonstrate that the B.1.1.7 and
183 B.1.617.2 isolates were more resistant to IFN β than the B.1 isolate (S6C Fig). Altogether, our
184 data demonstrate that the B.1, B.1.1.7, B.1.351, P.1 and B.1.617.2 isolates have evolved to resist
185 the IFN-I and IFN-III response.

186

187 **Discussion**

188 Numerous studies have shown that interferons are important for host defense against SARS-
189 CoV-2. This sarbecovirus is believed to have recently crossed the species barrier to humans,
190 either directly from bats or via an intermediate mammalian host(s) [34]. Here, we demonstrate
191 that SARS-CoV-2 has in fact evolved after host switching to become more resistant to human
192 interferons. Moreover, we establish an order of antiviral potency for the diverse type I and III
193 IFNs. IFN λ initially showed promise as an antiviral that can reduce inflammation [35], but our
194 data suggest that for SARS-CoV-2, higher doses of IFN λ may be needed to achieve a similar
195 antiviral effect *in vivo* as the IFN-Is. Nebulized IFN β showed potential as a therapeutic against
196 COVID-19 [11], and our data confirm IFN β is highly potent against SARS-CoV-2. However,
197 IFN β was also linked to pathogenic outcomes in chronic mucosal HIV-1 [23], murine LCMV
198 [36] and if administered late in mice, SARS-CoV-1 and MERS-CoV [37, 38] infection. We
199 previously reported that IFN β upregulated 2.4-fold more genes than individual IFN α subtypes,
200 suggesting that IFN β may induce more pleiotropic effects [23]. Among the IFN α subtypes,
201 IFN α 8 showed similar anti-SARS-CoV-2 potency as IFN β . IFN α 8 also exhibited high antiviral
202 activity against HIV-1 [3], raising its potential for treatment against both pandemic viruses.
203 Notably, IFN α 8 appeared to be an outlier in this regard, as the antiviral potencies of the IFN α
204 subtypes against SARS-CoV-2 and HIV-1 generally did not strongly correlate (Fig. 3C). IFN α 6
205 potently restricted HIV-1 [3, 4] but was one of the weakest IFN α subtypes against SARS-CoV-2.
206 Conversely, IFN α 5 strongly inhibited SARS-CoV-2, but weakly inhibited HIV-1 [3]. This lack
207 of correlation is a key point for future studies. Of note, the high potency of IFN α 5 and low
208 potency of IFN α 6 against an isolate of SARS-CoV-2 (not a variant of concern) were
209 corroborated by another group [39]. Collectively, these data strengthen the theory that diverse

210 IFNs may have evolved to restrict distinct virus families [2, 23]. The mechanisms underlying
211 these interesting qualitative differences remain unclear. While IFNAR signaling contributes to
212 antiviral potency [3, 4, 24], diverse IFNs may have distinct abilities to mobilize antiviral
213 effectors in specific cell types. Comparing the interferomes induced by distinct IFNs in lung
214 epithelial cells [39] may be useful in prioritizing further studies on this point.

215

216 Most significantly, our data reveal for the first time the concerning trend for SARS-CoV-2
217 variants emerging later in the pandemic – in the setting of prolific replication of the virus in
218 human populations – to resist the antiviral interferon response. Prior to the present work, the
219 emergence and fixation of variants was linked to enhanced viral infectivity and/or neutralizing
220 antibody evasion due to mutations in the Spike protein [13, 16-18, 40]. However, previous
221 studies with HIV-1 suggested that interferons also can shape the evolution of pandemic viruses
222 [41, 42]. In fact, SARS-CoV-2 infected individuals with either genetic defects in IFN signaling
223 [43] or IFN-reactive autoantibodies [44] had increased risk of developing severe COVID-19. As
224 interferons are critical in controlling early virus infection levels, IFN-resistant SARS-CoV-2
225 variants may produce higher viral loads that could in turn promote transmission and/or
226 exacerbate pathogenesis. Consistent with this hypothesis, some reports have linked B.1.1.7 with
227 increased viral loads [45, 46] and risk of death [47-49]. Notably, infection with B.1.617.2 may
228 yield even higher viral loads than that B.1.1.7 [50].

229

230 In addition to Spike, emerging variants exhibit mutations in nucleocapsid, membrane and
231 nonstructural proteins NSP3, NSP6 and NSP12 (S1 Table). In the case of some early pandemic
232 viruses that pre-dated the emergence of the variants of concern, these viral proteins were

233 reported to antagonize IFN signaling in cells [51-53]. To specifically map the virus mutations
234 driving IFN-I resistance in emerging variants, it will be important to generate recombinant
235 viruses to isolate specific mutations, singly or in combination, and individually test candidate
236 single viral protein antagonists as well. This would help to confirm, for example, that the D3L
237 mutation in the B.1.1.7 nucleocapsid may facilitate innate immune evasion by increasing the
238 expression of an interferon antagonist, ORF9b [33]. The nucleocapsid D3L mutation was not
239 observed in the B.1.351, P.1 and B.1.617.2 lineages (S1 Table), which exhibited IFN-I and IFN-
240 III resistance in our experiments. B.1.617.2 (delta) has now replaced B.1.1.7 (alpha) as the
241 dominant strain in many countries [27, 29], but delta did not seem to be any more interferon-
242 resistant than alpha in both A549-ACE2 and Calu-3 cells. Notably, the delta isolate we studied
243 here had a deletion in ORF7a, which may counteract interferon signaling [52]; this deletion was
244 not a cell culture artifact as it was also observed in the clinical isolate. Analysis of delta isolates
245 with or without the ORF7a deletion would be needed to determine whether innate immune
246 evasion may be a factor for why the delta VOC has overtaken other lineages. Future studies
247 should facilitate understanding the molecular mechanisms of interferon resistance, its
248 consequences for COVID-19 pathogenesis, and the development of novel therapies that augment
249 innate immune defenses against SARS-CoV-2.

250

251 Overall, the current study suggested a role for the innate immune response in driving the
252 evolution of SARS-CoV-2 that could have practical implications for interferon-based therapies.
253 Our findings reinforce the importance of continued full-genome surveillance of SARS-CoV-2,
254 and assessments of emerging variants not only for resistance to vaccine-elicited neutralizing
255 antibodies, but also for evasion of the host interferon response.

257 **Materials and Methods**

258

259 **Cell lines.** A549 cells were obtained from the American Type Culture Collection (ATCC) and
260 cultured in complete media containing F-12 Ham's media (Corning), 10% fetal bovine serum
261 (Atlanta Biologicals), 1% penicillin/streptomycin/glutamine (Corning). Calu-3 cells were also
262 obtained from ATCC and cultured in DMEM supplemented with 10% fetal bovine serum and
263 1% penicillin/streptomycin/glutamine (Corning). Both cell lines were maintained at 37°C 5%
264 CO₂. A549 cells were transduced with codon-optimized human ACE2 (Genscript) cloned into
265 pBABE-puro [54] (Addgene). To generate the A549-ACE2 stable cell line, 10⁷ HEK293T
266 (ATCC) cells in T-175 flasks were transiently co-transfected with 60 µg mixture of pBABE-
267 puro-ACE2, pUMVC, and pCMV-VSV-G at a 10:9:1 ratio using a calcium phosphate method
268 [55]. Forty-eight hours post transfection, the supernatant was collected, centrifuged at 1000 g
269 for 5 min and passed through a 0.45 µm syringe filter to remove cell debris. The filtered virus
270 was mixed with fresh media (30% vol/vol) that included polybrene (Sigma) at a 6 µg/ml final
271 concentration. The virus mixture was added into 6-well plates with 5 10⁵ A549 cells/well and
272 media was changed once more after 12 h. Transduced cells were selected in 0.5 µg/ml
273 puromycin for 72 h, and ACE2 expression was confirmed by flow cytometry, western blot and
274 susceptibility to HIV-1ΔEnv/SARS-CoV-2 Spike pseudovirions.

275

276 **Virus isolates.** All experiments with live SARS-CoV-2 were performed in a Biosafety Level-3
277 (BSL3) facility with powered air-purifying respirators at the University of Colorado Anschutz
278 Medical Campus. The SARS-CoV-2 stocks were obtained from BEI Resources
279 (www.beiresources.org). S1 Table provides detailed information on the source of the material,
280 the catalogue and lot numbers and virus sequence information of both the clinical and cultured

281 stocks. The viruses were propagated in human A549-ACE2 cells unless indicated and harvested
282 by 72 h to minimize mutations that can occur during passage in cell culture, which were
283 documented particularly in nonhuman primate (Vero) or non-alveolar type II (293T) cell lines
284 [56]. The virus stocks had comparable titers $>10^6$ TCID₅₀/ml (S1A Fig) except for the two
285 B.1.1.7 strains (CA_CDC_5574/2020 and England/204820464/2020). The contents of the entire
286 vial (~0.5 ml) were inoculated into 3 T-75 flasks containing $3 \cdot 10^6$ A549-ACE2 cells, except for
287 B.1.1.7 which was inoculated into 1 T-75 flask. The supernatants were collected and spun at
288 2700 g for 5 min to remove cell debris, and frozen at -80°C. The A549-amplified stocks were
289 titered according to the proposed assay format (S1B Fig, Fig 2A). Briefly, $2.5 \cdot 10^4$ A549-ACE2
290 cells were plated per well in a 48-well plate overnight. The next day, the cells were infected with
291 300, 30, 3, 0.3, 0.03 and 0.003 μ l (serial 10-fold dilution) of amplified virus stock in 300 μ l final
292 volume of media for 2 h. The virus was washed twice with PBS, and 500 μ l of complete media
293 with the corresponding IFN concentrations were added. After 24 h, supernatants were collected,
294 and cell debris was removed by centrifugation at 3200 g for 5 min.

295

296 **Cell viability.** To evaluate if the IFN doses affected cell viability, we utilized an MTT assay.
297 $1.5 \cdot 10^4$ A549-ACE2 cells were plated per well in a 96-well plate and treated with 2000 pM
298 IFN λ 1, 2 pM IFN λ 1, 200 pM IFN β , 2 pM IFN β or untreated. Eight replicates were used per
299 treatment group. As a positive control for cell death, the same number of cells were treated with
300 30% DMSO. 36 hours after treatment, cell proliferation was assessed using the Vybrant MTT
301 Cell Proliferation Assay Kit (Invitrogen). Media was completely removed from cells and
302 replaced with 100 μ l of fresh growth media. 10 μ l of 12 mM MTT stock solution was added per
303 well and cells were incubated at 37°C for 4 h. 100 μ l SDS-HCl solution was added to each well

304 and mixed thoroughly. After an additional 3 h incubation at 37°C, the absorbance was measured
305 at 570 nm and blank corrected to a media only control.

306

307 **SARS-CoV-2 quantitative PCR.** For rapid and robust assessments of viral replication, we
308 utilized a real-time quantitative PCR (qPCR) approach. This assay would require less handling of
309 infectious, potentially high-titer SARS-CoV-2 in the BSL3 compared to a VeroE6 plaque assay,
310 as the supernatants can be directly placed in lysis buffer containing guanidinium thiocyanate that
311 would inactivate the virus by at least 4-5 log₁₀ [57]. Importantly, residual IFNs in the culture
312 supernatant could further inhibit virus infection in the VeroE6 plaque assay, compromising the
313 infectious titer read-outs. To measure SARS-CoV-2 levels, total RNA was extracted from 100 µl
314 of culture supernatant using the E.Z.N.A Total RNA Kit I (Omega Bio-Tek) and eluted in 50 µl
315 of RNase-free water. 5 µl of this extract was used for qPCR. Official CDC SARS-CoV-2 N1
316 gene primers and TaqMan probe set were used [58] with the Luna Universal Probe One-Step
317 RT-qPCR Kit (New England Biolabs):

318 Forward primer: GACCCCAAAATCAGCGAAAT

319 Reverse primer: TCTGGTTACTGCCAGTTGAATCTG

320 TaqMan probe: FAM-ACCCCGCATTACGTTGGTGGACC-TAMRA

321 The sequence of the primers and probes were conserved against the 7 SARS-CoV-2 lineages that
322 were investigated. The real-time qPCR reaction was run on a Bio-Rad CFX96 real-time
323 thermocycler under the following conditions: 55°C 10 mins for reverse transcription, then 95°C
324 1 min followed by 40 cycles of 95°C 10s and 60°C 30s. The absolute quantification of the N1
325 copy number was interpolated using a standard curve with 10⁷-10¹ serial 10-fold dilution of a
326 control plasmid (nCoV-CDC-Control Plasmid, Eurofins).

327 **VeroE6 Plaque Assay.** Virus stocks with a pre-determined virus copy number were evaluated
328 in a conventional VeroE6 plaque assay to determine if the virus titers obtained using both
329 methods correlate. 4 10^5 VeroE6 cells (ATCC) were plated in 6-well plates and allowed to
330 adhere overnight at 37°C. Cells were washed once with PBS and infected with 1 ml of viral
331 stocks serially diluted in 2 MEM complete media (10% FBS, 20 mM HEPES, 2 Pen-Step, 2
332 NEAA and 2 Sodium Pyruvate) for 1 hr at 37°C. After infection, 1 ml of sterile 2.5% cellulose
333 overlay solution (Sigma, Cat. No. 435244-250G) was added to each well and mixed thoroughly.
334 Cells were incubated at 37°C for an additional 48 hr before the media/overlay was removed and
335 the cells fixed in 4% paraformaldehyde (PFA) for 10 min at room temperature. The PFA was
336 removed and the cells were stained with 1% crystal violet in ethanol for 1 minute and washed
337 three times with distilled water. Plaques were manually counted from each well.

338

339 **Immunofluorescence Assay.** Primary human airway epithelial cells fully differentiated in air-
340 liquid interface cultures [59] were infected with different SARS-CoV-2 variants with or without
341 IFN β . The apical surface was washed with culture medium daily for quantitative PCR. At 96 h
342 post-infection, the cultures were fixed with 4% PFA and wholmount labeled with anti-Spike
343 antibody (Clone ID007, Cat. No. 40150-R007, Sino Biological) followed by Alexa-Dye
344 conjugated secondary antibody. An LSM 900 confocal microscope (Zeiss) was used to generate
345 composite images of the entire culture surface. Spike+ cells were enumerated using the Cell
346 Counter plugin in the ImageJ Software (NIH).

347

348 **Antiviral inhibition assay.** We used a non-saturating dose of the amplified virus stock for the
349 IFN inhibition assays. These titers were expected to yield $\sim 10^5$ copies per 5 μ l input RNA extract

350 (S1B Fig). Recombinant IFNs were obtained from PBL Assay Science. These recombinant IFNs
351 were assayed to be >95% pure by SDS-PAGE according to the manufacturer. In addition to the
352 IFN-Is (12 IFN α subtypes, IFN β and IFN ω), we also evaluated 3 IFN λ subtypes (IFN λ 1, IFN λ 2,
353 IFN λ 3). To normalize the IFNs, we used molar concentrations [23] instead of international units
354 (IU), as IU values were derived from inhibition of encephalomyocarditis virus, which may not
355 be relevant to SARS-CoV-2. Importantly, molar concentrations were used to normalize the
356 relative signaling potencies of the IFN α subtypes and IFN β [23, 24]. To find a suitable dose to
357 screen 17 IFNs in parallel, we performed a dose-titration experiment of the USA-WA1/2020
358 strain with IFN β and IFN λ 1. A dose of 2 pM allowed for maximum discrimination of the
359 antiviral potency IFN β versus IFN λ 1 (S1C Fig). Thus, this dose should be within the dynamic
360 range of inhibition of the diverse IFNs investigated. Serial 10-fold dilutions of IFN β and IFN λ 1
361 were also used in follow-up experiments. Thus, in 48-well plates, we pre-incubated $2.5 \cdot 10^4$
362 A549-ACE2 cells with the IFNs for 18 h, then infected with the A549-amplified virus stock for 2
363 h. After two washes with PBS, 500 μ l complete media containing the corresponding IFNs were
364 added. The cultures were incubated for another 24 h, after which, supernatants were harvested
365 for RNA extraction and qPCR analysis. A similar procedure was employed for Calu-3 cells,
366 except that IFN λ 1 was replenished at 2 dpi and supernatants harvested at day 3.
367

368 **Statistical analyses.** Data were analyzed using GraphPad Prism 8. Differences between the IFNs
369 were tested using a nonparametric two-way analysis of variance (ANOVA) followed by a
370 multiple comparison using the Friedman test. Pearson correlation coefficients (R^2) values were
371 computed for linear regression analyses. Paired analysis of two isolates against multiple IFNs
372 were performed using a nonparametric, two-tailed Wilcoxon matched-pairs rank test. Differences

373 with $p < 0.05$ were considered significant. Nonlinear regression curves were used to fit using
374 either a one-site total or two-phase exponential decay equation on log-transformed data.

375

376

377 **Acknowledgments**

378 We thank Cara Wilson, Ulf Dittmer and Kathrin Gibbert for scientific advice; Mercedes Rincon
379 and Elan Eisenmesser for assistance with construction and characterization of the A549-ACE2
380 cells; Zach Wilson, Jill Garvey, Stephanie Torres-Nemeti, Brett Haltiwanger and Marcia
381 Finucane for Biosafety Level-3 infrastructure support; and Roman Wölfel, Rosina Ehmann,
382 Adolfo García-Sastre, Alex Sigal, Túlio de Oliveira, Bassam Hallis, Matsuyo Takayama-Ito,
383 Richard Webby, Anami Patel, Cathleen Seager, BEI Resources (NIAID) and the CDC for the
384 SARS-CoV-2 isolates.

385

386 **Funding**

387 This work was supported by the Division of Infectious Diseases, Department of Medicine,
388 University of Colorado (MLS and EMP), the National Institutes of Health R01 AI134220
389 (MLS), and the Intramural Research Program at the National Institute of Allergy and Infectious
390 Diseases, National Institutes of Health (KJH). The funders had no role in study design, data
391 collection and analysis, decision to publish, or preparation of the manuscript.

392

393 **Figures**

394 **Figure 1. Selection of SARS-CoV-2 strains for IFN sensitivity studies.** (A) Global
395 distribution of SARS-CoV-2 clades. GISAID.org plotted the proportion of deposited sequences
396 in designated clades against collection dates. The six isolates chosen are noted by colored dots.
397 (B) SARS-CoV-2 strains selected for this study included representatives of lineages A, B, B.1,
398 B.1.351 and B.1.1.7 (S1 Table). Lineage P.1 (which branched off from lineage B.1.1.28) and
399 B.1.617.2 were added after the initial manuscript submission; and was evaluated for IFN β and
400 IFN λ 1 sensitivity. Lineage B isolates encode the D614G mutation associated with increased
401 transmissibility. Note that the B.1.1.7 strain was later updated to belong to the GISAID clade,
402 'GRY'. *Amino acid mutations were relative to the reference hCOV-19/Wuhan/WIV04/2019
403 sequence.

404

405 **Figure 2. Sensitivity of SARS-CoV-2 strains to IFN-I and IFN-III interferons.** (A) Antiviral
406 assay using recombinant IFNs (2 pM) in A549-ACE2 cells. The red line corresponds to the
407 qPCR detection limit (90 copies/reaction, or 1.8×10^4 copies/ml). (B) Viral copy numbers in
408 D614G+ isolates, showing a similar rank-order of IFNs from least to most potent. (C) The
409 average fold-inhibition relative to mock for lineage B, B.1, B.1.351 and B.1.1.7 isolates are
410 shown. The most potent IFNs are shown top to bottom. For all panels, bars and error bars
411 correspond to means and standard deviations.

412

413 **Figure 3. Correlation between SARS-CoV-2 inhibition and biological properties of IFN α**
414 **subtypes.** Log-transformed IFN-inhibition values relative to mock for the 5 different SARS-
415 CoV-2 strains were compared to previously published values on (A) 50% effective

416 concentrations in the iLite assay, a reporter cell line encoding the IFN sensitive response element
417 of *ISG15* linked to firefly luciferase [23]; (B) IFNAR2 subunit binding affinity, as measured by
418 surface plasmon resonance by the Schreiber group [24]; and (C) HIV-1 inhibition values, based
419 on % inhibition of HIV-1 p24+ gut lymphocytes relative to mock as measured by flow cytometry
420 [3]. Each dot corresponds to an IFN α subtype. Linear regression was performed using GraphPad
421 Prism 8. Significant correlations ($p<0.05$) were highlighted with a red best-fit line; those that
422 were trending ($p<0.1$) had a gray, dotted best-fit line.

423

424 **Figure 4. Increased IFN-I resistance of emerging SARS-CoV-2 variants.** (A) Heatmap of
425 fold-inhibition of representative strains from the lineages noted. Colors were graded on a log-
426 scale from highest inhibition (yellow) to no inhibition (black). Comparison of IFN-I sensitivities
427 between (B) lineage A and B isolates; (C) lineage B versus B.1, B.1.351 and B.1.1.7 and (D)
428 lineage A versus B.1, B.1.351 and B.1.1.7. The mean fold-inhibition values relative to mock
429 were compared in a pairwise fashion for the 14 IFN-Is. In (C) and (D), the average fold-
430 inhibition values were noted. Differences were evaluated using a nonparametric, two-tailed
431 Wilcoxon matched-pairs signed rank test. NS, not significant; ****, $p<0.0001$.

432

433 **Figure 5. Dose-titration of ancestral lineage B versus four variants of concern against IFN β**
434 **and IFN λ 1.** Data from four separate experiments (panels A-D) are shown. (A) Dose-titration of
435 IFN β and IFN λ 1 against lineage B (Germany/BavPat1/2020) versus B.1.1.7 (alpha) isolates. In
436 addition to USA/CA_CDC_5574/2020, we also evaluated a second B.1.1.7 isolate from the
437 United Kingdom (UK), England/204820464/2020. *The value at 200 pM IFN λ 1 for the lineage
438 B isolate was 0.54, precluding efforts for finding a best-fit curve for IC50 determination; this

439 datapoint was therefore not included in the curve fitting. (B) IC50 comparison between a lineage
440 B (Germany/BavPat1/2020) and a B.1.351 (beta) isolate (South Africa/KRISP-EC-
441 K005321/2020). (C) IC50 comparison between a lineage B isolate (Germany/BavPat1/2020) and
442 a P.1 (gamma) isolate (Japan/TY7-503/2021). (D) IC50 comparison between a lineage B isolate
443 (Germany/BavPat1/2020) and a B.1.617.2 (delta) isolate (USA/PHC658/2021). For all panels,
444 A549-ACE2 cells were pre-treated with serial 10-fold dilutions of IFNs for 18 h in triplicate and
445 then infected with SARS-CoV-2. Supernatants were collected after 24 h, SARS-CoV-2 N1 copy
446 numbers were determined by qPCR in triplicate, and then the mean copy numbers were
447 normalized against mock as 100%. Error bars correspond to standard deviations. Non-linear best-
448 fit regression curves of mean normalized infection levels were used to interpolate 50% inhibitory
449 concentrations (green dotted lines).

450

451 **References**

- 452 1. Pestka S, Krause CD, Walter MR. Interferons, interferon-like cytokines, and their receptors. 453 *Immunol Rev.* 2004;202:8-32. Epub 2004/11/18.
- 454 2. Gibbert K, Schlaak JF, Yang D, Dittmer U. IFN-alpha subtypes: distinct biological activities 455 in anti-viral therapy. *British journal of pharmacology.* 2013;168(5):1048-58.
- 456 3. Harper MS, Guo K, Gibbert K, Lee EJ, Dillon SM, Barrett BS, et al. Interferon-alpha 457 Subtypes in an Ex Vivo Model of Acute HIV-1 Infection: Expression, Potency and Effector 458 Mechanisms. *PLoS pathogens.* 2015;11(11):e1005254.
- 459 4. Schlaepfer E, Fahrny A, Gruenbach M, Kuster SP, Simon V, Schreiber G, et al. Dose- 460 Dependent Differences in HIV Inhibition by Different Interferon Alpha Subtypes While 461 Having Overall Similar Biologic Effects. *mSphere.* 2019;4(1). Epub 2019/02/15.
- 462 5. Lavender KJ, Gibbert K, Peterson KE, Van Dis E, Francois S, Woods T, et al. Interferon 463 Alpha Subtype-Specific Suppression of HIV-1 Infection In Vivo. *Journal of virology.* 464 2016;90(13):6001-13.
- 465 6. Matos ADR, Wunderlich K, Schloer S, Schughart K, Geffers R, Seders M, et al. Antiviral 466 potential of human IFN-alpha subtypes against influenza A H3N2 infection in human lung 467 explants reveals subtype-specific activities. *Emerg Microbes Infect.* 2019;8(1):1763-76.
- 468 7. Vanderheiden A, Ralfs P, Chirkova T, Upadhyay AA, Zimmerman MG, Bedoya S, et al. 469 Type I and Type III Interferons Restrict SARS-CoV-2 Infection of Human Airway Epithelial 470 Cultures. *Journal of virology.* 2020;94(19). Epub 2020/07/24.
- 471 8. Felgenhauer U, Schoen A, Gad HH, Hartmann R, Schaubmar AR, Failing K, et al. Inhibition 472 of SARS-CoV-2 by type I and type III interferons. *The Journal of biological chemistry.* 473 2020;295(41):13958-64. Epub 2020/06/27.
- 474 9. Nchioua R, Kmiec D, Muller JA, Conzelmann C, Gross R, Swanson CM, et al. SARS-CoV-2 475 Is Restricted by Zinc Finger Antiviral Protein despite Preadaptation to the Low-CpG 476 Environment in Humans. *mBio.* 2020;11(5). Epub 2020/10/18.
- 477 10. Wang N, Zhan Y, Zhu L, Hou Z, Liu F, Song P, et al. Retrospective Multicenter Cohort 478 Study Shows Early Interferon Therapy Is Associated with Favorable Clinical Responses in 479 COVID-19 Patients. *Cell host & microbe.* 2020;28(3):455-64 e2. Epub 2020/07/25.
- 480 11. Monk PD, Marsden RJ, Tear VJ, Brookes J, Batten TN, Mankowski M, et al. Safety and 481 efficacy of inhaled nebulised interferon beta-1a (SNG001) for treatment of SARS-CoV-2 482 infection: a randomised, double-blind, placebo-controlled, phase 2 trial. *Lancet Respir Med.* 483 2020. Epub 2020/11/16.
- 484 12. Shalhoub S. Interferon beta-1b for COVID-19. *Lancet.* 2020;395(10238):1670-1. Epub 485 2020/05/14.
- 486 13. Rambaut A, Holmes EC, O'Toole A, Hill V, McCrone JT, Ruis C, et al. A dynamic 487 nomenclature proposal for SARS-CoV-2 lineages to assist genomic epidemiology. *Nat 488 Microbiol.* 2020;5(11):1403-7. Epub 2020/07/17.
- 489 14. Zhou P, Yang XL, Wang XG, Hu B, Zhang L, Zhang W, et al. A pneumonia outbreak 490 associated with a new coronavirus of probable bat origin. *Nature.* 2020;579(7798):270-3.

491 15. Worobey M, Pekar J, Larsen BB, Nelson MI, Hill V, Joy JB, et al. The emergence of SARS-
492 CoV-2 in Europe and North America. *Science* (New York, NY. 2020;370(6516):564-70.
493 Epub 2020/09/12.

494 16. Korber B, Fischer WM, Gnanakaran S, Yoon H, Theiler J, Abfalsterer W, et al. Tracking
495 Changes in SARS-CoV-2 Spike: Evidence that D614G Increases Infectivity of the COVID-
496 Virus. *Cell*. 2020;182(4):812-27 e19. Epub 2020/07/23.

497 17. Plante JA, Liu Y, Liu J, Xia H, Johnson BA, Lokugamage KG, et al. Spike mutation D614G
498 alters SARS-CoV-2 fitness. *Nature*. 2020. Epub 2020/10/28.

499 18. Hou YJ, Chiba S, Halfmann P, Ehre C, Kuroda M, Dinnon KH, 3rd, et al. SARS-CoV-2
500 D614G variant exhibits efficient replication ex vivo and transmission in vivo. *Science* (New
501 York, NY. 2020;370(6523):1464-8. Epub 2020/11/14.

502 19. Gonzalez-Reiche AS, Hernandez MM, Sullivan MJ, Ciferri B, Alshammary H, Obla A, et al.
503 Introductions and early spread of SARS-CoV-2 in the New York City area. *Science* (New
504 York, NY. 2020;369(6501):297-301. Epub 2020/05/31.

505 20. Wibmer CK, Ayres F, Hermanus T, Madzivhandila M, Kgagudi P, Oosthuysen B, et al.
506 SARS-CoV-2 501Y.V2 escapes neutralization by South African COVID-19 donor plasma.
507 *Nature medicine*. 2021. Epub 2021/03/04.

508 21. Wang P, Nair MS, Liu L, Iketani S, Luo Y, Guo Y, et al. Antibody Resistance of SARS-
509 CoV-2 Variants B.1.351 and B.1.1.7. *Nature*. 2021. Epub 2021/03/09.

510 22. Galloway SE, Paul P, MacCannell DR, Johansson MA, Brooks JT, MacNeil A, et al.
511 Emergence of SARS-CoV-2 B.1.1.7 Lineage - United States, December 29, 2020-January
512 12, 2021. *MMWR Morb Mortal Wkly Rep*. 2021;70(3):95-9. Epub 2021/01/22.

513 23. Guo K, Shen G, Kibbie J, Gonzalez T, Dillon SM, Smith HA, et al. Qualitative Differences
514 Between the IFNalpha subtypes and IFNbta Influence Chronic Mucosal HIV-1
515 Pathogenesis. *PLoS pathogens*. 2020;16(10):e1008986. Epub 2020/10/17.

516 24. Lavoie TB, Kalie E, Crisafulli-Cabatu S, Abramovich R, DiGioia G, Moolchan K, et al.
517 Binding and activity of all human alpha interferon subtypes. *Cytokine*. 2011;56(2):282-9.

518 25. Faria NR, Mellan TA, Whittaker C, Claro IM, Candido DDS, Mishra S, et al. Genomics and
519 epidemiology of the P.1 SARS-CoV-2 lineage in Manaus, Brazil. *Science* (New York, NY.
520 2021;372(6544):815-21. Epub 2021/04/16.

521 26. Naveca FG, Nascimento V, de Souza VC, Corado AL, Nascimento F, Silva G, et al. COVID-
522 19 in Amazonas, Brazil, was driven by the persistence of endemic lineages and P.1
523 emergence. *Nature medicine*. 2021. Epub 2021/05/27.

524 27. Mlcochova P, Kemp S, Dhar MS, Papa G, Meng B, Mishra S, et al. SARS-CoV-2 B.1.617.2
525 Delta variant emergence and vaccine breakthrough. Research Square Platform LLC.

526 28. Singh J, Rahman SA, Ehtesham NZ, Hira S, Hasnain SE. SARS-CoV-2 variants of concern
527 are emerging in India. *Nature medicine*. 2021;27(7):1131-3. Epub 2021/05/29.

528 29. Monitoring Variant Proportions [Internet]. 2021. Available from:
529 <https://covid.cdc.gov/covid-data-tracker/#variant-proportions>.

530 30. Chia PY, Ong SWX, Chiew CJ, Ang LW, Chavatte JM, Mak TM, et al. Virological and
531 serological kinetics of SARS-CoV-2 Delta variant vaccine-breakthrough infections: a multi-
532 center cohort study. medRxiv. 2021.

533 31. Brown CM, Vostok J, Johnson H, Burns M, Gharpure R, Sami S, et al. Outbreak of SARS-
534 CoV-2 Infections, Including COVID-19 Vaccine Breakthrough Infections, Associated with
535 Large Public Gatherings - Barnstable County, Massachusetts, July 2021. MMWR Morb
536 Mortal Wkly Rep. 2021;70(31):1059-62. Epub 2021/08/06.

537 32. Guo K, Barrett BS, Mickens KL, Hasenkrug KJ, Santiago ML. Interferon Resistance of
538 Emerging SARS-CoV-2 Variants. bioRxiv. 2021. Epub 2021/03/25.

539 33. Thorne LG, Bouhaddou M, Reuschl AK, Zuliani-Alvarez L, Polacco B, Pelin A, et al.
540 Evolution of enhanced innate immune evasion by the SARS-CoV-2 B.1.1.7 UK variant.
541 bioRxiv. 2021. Epub 2021/06/16.

542 34. Holmes EC, Goldstein SA, Rasmussen AL, Robertson DL, Crits-Christoph A, Wertheim JO,
543 et al. The origins of SARS-CoV-2: A critical review. Cell. 2021. Epub 2021/09/05.

544 35. Davidson S, McCabe TM, Crotta S, Gad HH, Hessel EM, Beinke S, et al. IFNlambda is a
545 potent anti-influenza therapeutic without the inflammatory side effects of IFNalpha
546 treatment. EMBO molecular medicine. 2016;8(9):1099-112.

547 36. Ng CT, Sullivan BM, Teijaro JR, Lee AM, Welch M, Rice S, et al. Blockade of interferon
548 Beta, but not interferon alpha, signaling controls persistent viral infection. Cell host &
549 microbe. 2015;17(5):653-61.

550 37. Channappanavar R, Fehr AR, Zheng J, Wohlford-Lenane C, Abrahante JE, Mack M, et al.
551 IFN-I response timing relative to virus replication determines MERS coronavirus infection
552 outcomes. J Clin Invest. 2019;130:3625-39.

553 38. Channappanavar R, Fehr AR, Vijay R, Mack M, Zhao J, Meyerholz DK, et al. Dysregulated
554 Type I Interferon and Inflammatory Monocyte-Macrophage Responses Cause Lethal
555 Pneumonia in SARS-CoV-Infected Mice. Cell host & microbe. 2016;19(2):181-93.

556 39. Schuhenn J, Meister TL, Todt D, Bracht T, Schork K, Billaud J-N, et al. Differential
557 interferon-alpha subtype immune signatures suppress SARS-CoV-2 infection. BioRxiv.
558 2021.

559 40. Weisblum Y, Schmidt F, Zhang F, DaSilva J, Poston D, Lorenzi JC, et al. Escape from
560 neutralizing antibodies by SARS-CoV-2 spike protein variants. Elife. 2020;9. Epub
561 2020/10/29.

562 41. Iyer SS, Bibollet-Ruche F, Sherrill-Mix S, Learn GH, Plenderleith L, Smith AG, et al.
563 Resistance to type 1 interferons is a major determinant of HIV-1 transmission fitness.
564 Proceedings of the National Academy of Sciences of the United States of America.
565 2017;114(4):E590-E9. Epub 2017/01/11.

566 42. Parrish NF, Gao F, Li H, Giorgi EE, Barbian HJ, Parrish EH, et al. Phenotypic properties of
567 transmitted founder HIV-1. Proceedings of the National Academy of Sciences of the United
568 States of America. 2013;110(17):6626-33.

569 43. Zhang Q, Bastard P, Liu Z, Le Pen J, Moncada-Velez M, Chen J, et al. Inborn errors of type I
570 IFN immunity in patients with life-threatening COVID-19. *Science* (New York, NY.
571 2020;370(6515). Epub 2020/09/26.

572 44. Bastard P, Rosen LB, Zhang Q, Michailidis E, Hoffmann HH, Zhang Y, et al. Autoantibodies
573 against type I IFNs in patients with life-threatening COVID-19. *Science* (New York, NY.
574 2020;370(6515). Epub 2020/09/26.

575 45. Kidd M, Richter A, Best A, Cumley N, Mirza J, Percival B, et al. S-variant SARS-CoV-2
576 lineage B1.1.7 is associated with significantly higher viral loads in samples tested by
577 ThermoFisher TaqPath RT-qPCR. *The Journal of infectious diseases*. 2021. Epub
578 2021/02/14.

579 46. Frampton D, Rampling T, Cross A, Bailey H, Heaney J, Byott M, et al. Genomic
580 characteristics and clinical effect of the emergent SARS-CoV-2 B.1.1.7 lineage in London,
581 UK: a whole-genome sequencing and hospital-based cohort study. *Lancet Infectious
582 Diseases*. 2021.

583 47. Grint DJ, Wing K, Williamson E, McDonald HI, Bhaskaran K, Evans D, et al. Case fatality
584 risk of the SARS-CoV-2 variant of concern B.1.1.7 in England, 16 November to 5 February.
585 *Euro Surveill*. 2021;26(11). Epub 2021/03/20.

586 48. Davies NG, Jarvis CI, Group CC-W, Edmunds WJ, Jewell NP, Diaz-Ordaz K, et al. Increased mortality in community-tested cases of SARS-CoV-2 lineage B.1.1.7. *Nature*.
587 2021. Epub 2021/03/17.

588 49. Challen R, Brooks-Pollock E, Read JM, Dyson L, Tsaneva-Atanasova K, Danon L. Risk of
589 mortality in patients infected with SARS-CoV-2 variant of concern 202012/1: matched
590 cohort study. *BMJ*. 2021;372:n579. Epub 2021/03/11.

591 50. Ong SWX, Chiew CJ, Ang LW, Mak TM, Cui L, Toh M, et al. Clinical and virological
592 features of SARS-CoV-2 variants of concern: a retrospective cohort study comparing B.1.1.7
593 (Alpha), B.1.315 (Beta), and B.1.617.2 (Delta). *Clin Infect Dis*. 2021. Epub 2021/08/24.

594 51. Lei X, Dong X, Ma R, Wang W, Xiao X, Tian Z, et al. Activation and evasion of type I
595 interferon responses by SARS-CoV-2. *Nat Commun*. 2020;11(1):3810. Epub 2020/08/01.

596 52. Xia H, Cao Z, Xie X, Zhang X, Chen JY, Wang H, et al. Evasion of Type I Interferon by
597 SARS-CoV-2. *Cell reports*. 2020;33(1):108234. Epub 2020/09/28.

598 53. Mu J, Fang Y, Yang Q, Shu T, Wang A, Huang M, et al. SARS-CoV-2 N protein antagonizes
599 type I interferon signaling by suppressing phosphorylation and nuclear translocation of
600 STAT1 and STAT2. *Cell Discov*. 2020;6:65. Epub 2020/09/22.

601 54. Morgenstern JP, Land H. Advanced mammalian gene transfer: high titre retroviral vectors
602 with multiple drug selection markers and a complementary helper-free packaging cell line.
603 *Nucleic acids research*. 1990;18(12):3587-96. Epub 1990/06/25.

604 55. Dillon SM, Guo K, Castleman MJ, Santiago ML, Wilson CC. Quantifying HIV-1-Mediated
605 Gut CD4+ T Cell Death in the Lamina Propria Aggregate Culture (LPAC) Model Bio-
606 Protocol. 2020;10(2).

608 56. Sasaki M, Uemura K, Sato A, Toba S, Sanaki T, Maenaka K, et al. SARS-CoV-2 variants
609 with mutations at the S1/S2 cleavage site are generated in vitro during propagation in
610 TMPRSS2-deficient cells. *PLoS pathogens*. 2021;17(1):e1009233. Epub 2021/01/22.

611 57. Pastorino B, Touret F, Gilles M, Luciani L, de Lamballerie X, Charrel RN. Evaluation of
612 Chemical Protocols for Inactivating SARS-CoV-2 Infectious Samples. *Viruses*. 2020;12(6).
613 Epub 2020/06/12.

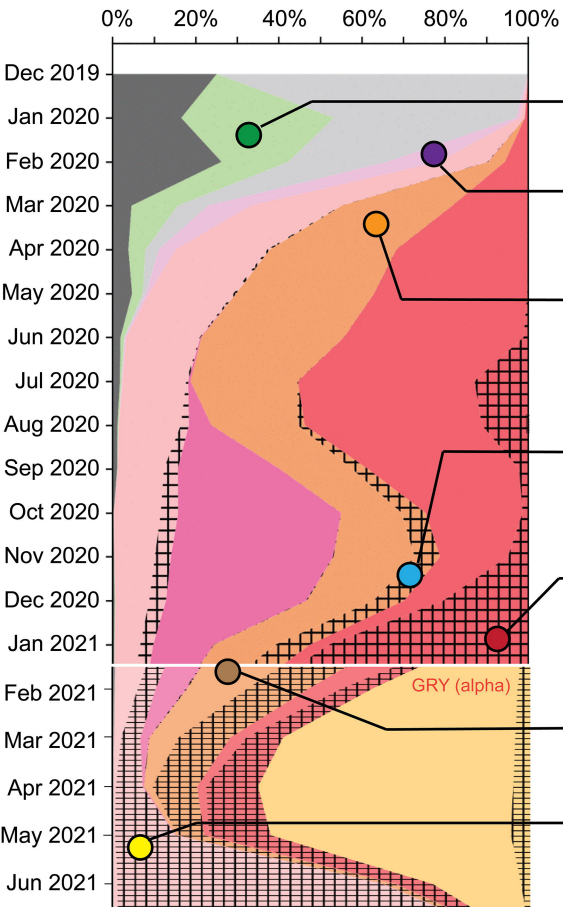
614 58. CDC. Research Use Only 2019-Novel Coronavirus (2019-nCoV) Real-time RT-PCR Primers
615 and Probes. <https://www.cdc.gov/coronavirus/2019-ncov/lab/rt-pcr-panel-primer-probes.html>. 2020.

617 59. Robinot R, Hubert M, de Melo GD, Lazarini F, Bruel T, Smith N, et al. SARS-CoV-2
618 infection induces the dedifferentiation of multiciliated cells and impairs mucociliary
619 clearance. *Nat Commun*. 2021;12(1):4354. Epub 2021/07/18.

620

A Global Clade Distribution

(GISAID.org, as of 8/12/2021)

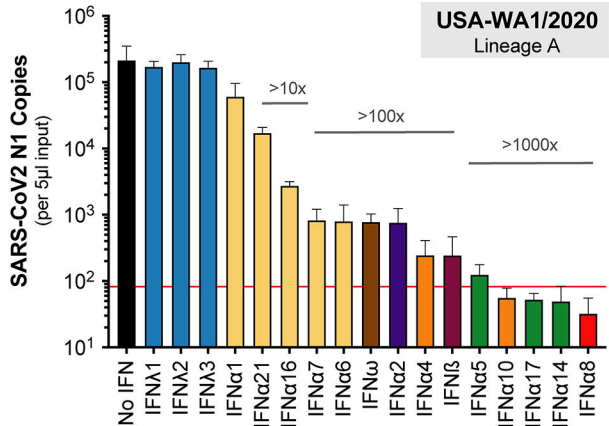
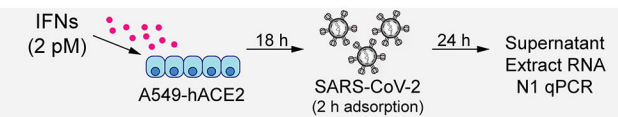
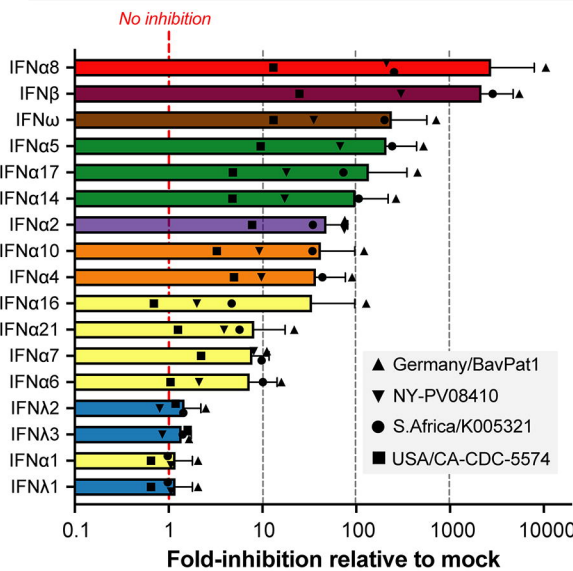
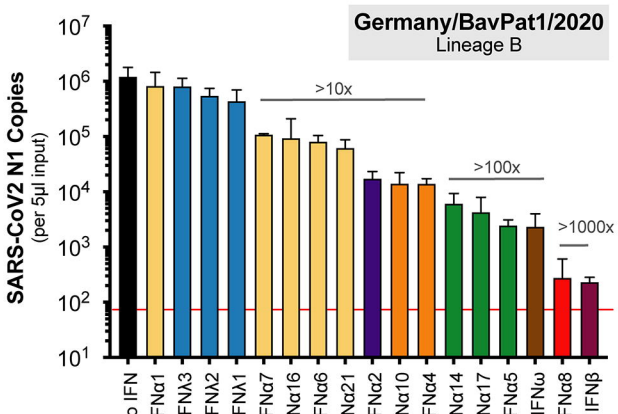
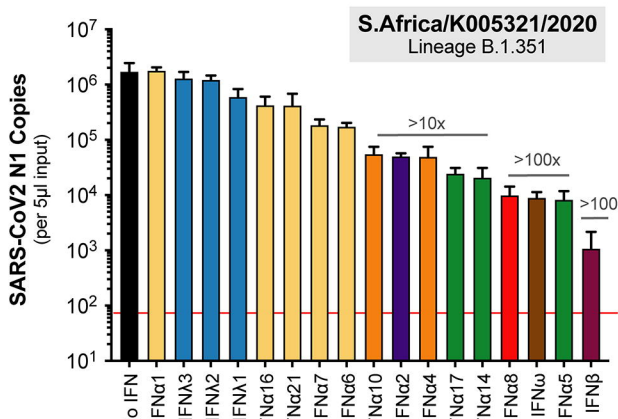
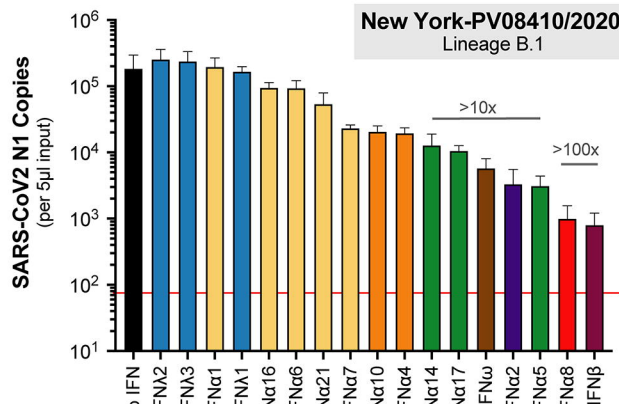
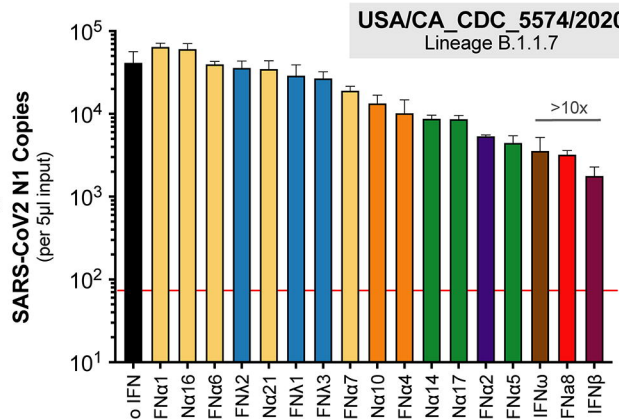
**B Isolates tested for IFN sensitivity**

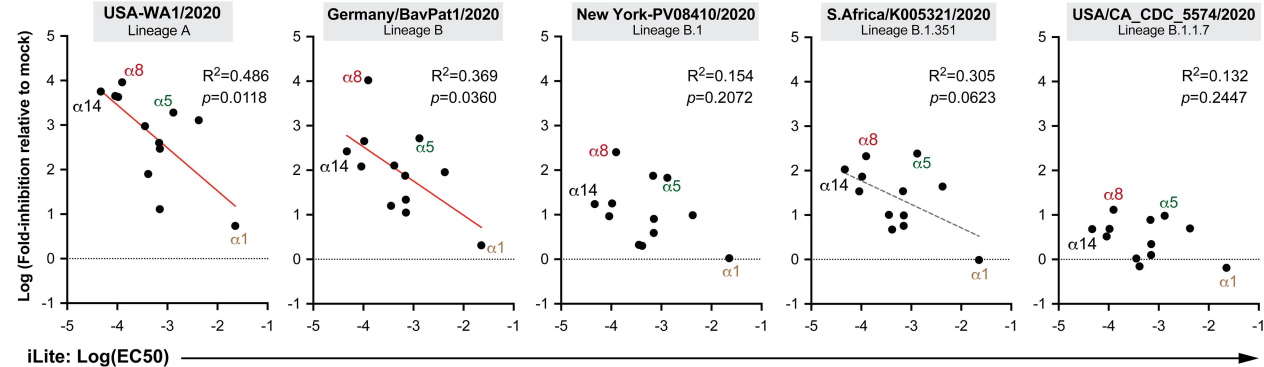
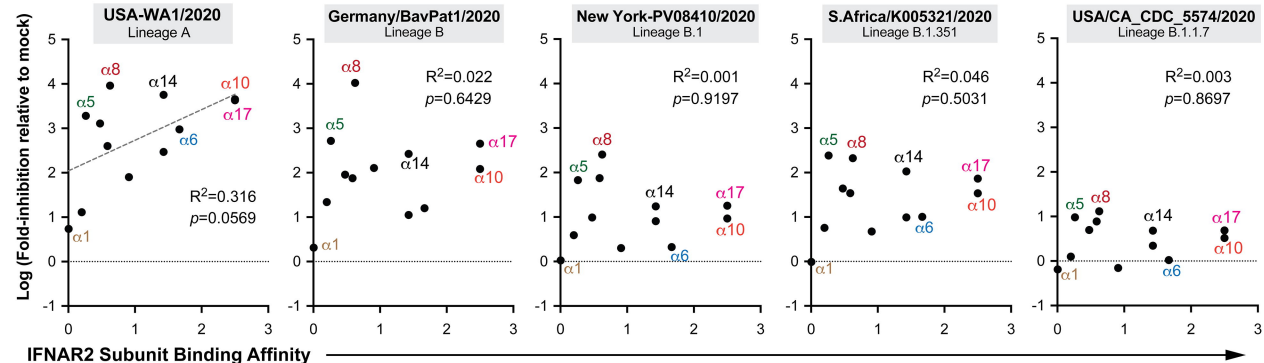
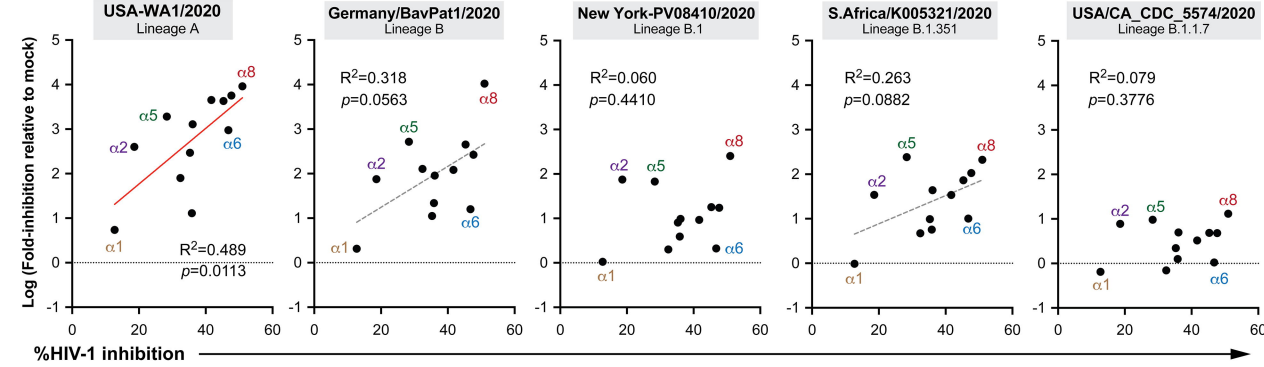
SARS-CoV-2 Isolate Name	Notable Mutations in Spike (and other genes)*
USA-WA1/2020	None (NS8 L84S)
Lineage: A	
Germany/BavPat1/2020	D614G (no mutations in other genes)
Lineage: B	
New York-PV08410/2020	D614G (NSP2 T85I, NSP12 P323L, NS3 Q57H)
Lineage: B.1	
South Africa/KRISP-EC-K005321/2020	D614G, N501Y, E484K + many others
Lineage: B.1.351	
(Beta)	
USA/CA_CDC_5574/2020	D614G, N501Y + many others
England/204820464/2020	
Lineage: B.1.1.7	
(Alpha)	
Feb 2021	GRY (alpha)
Japan/TY-503/2021 (Brazil P.1)	D614G, N501Y, E484K + many others
Lineage: P.1	
(Gamma)	
USA/PHC658/2021	D614G, L452R + many others
Lineage: B.1.617.2	
(Delta)	

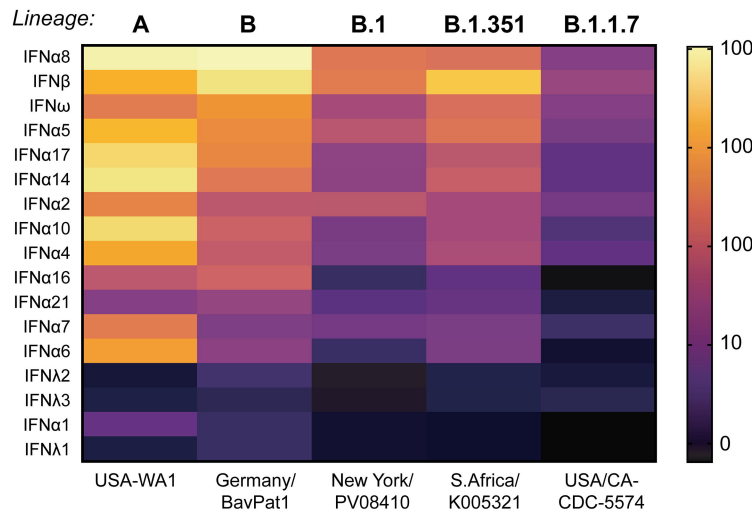
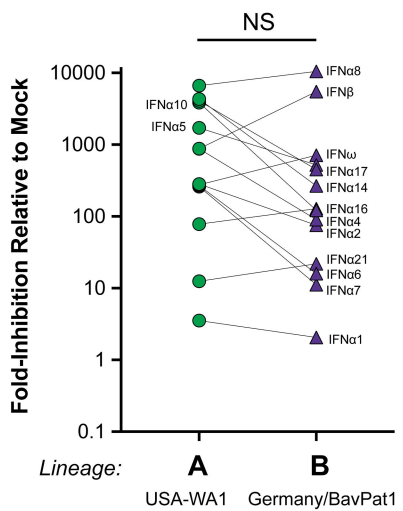
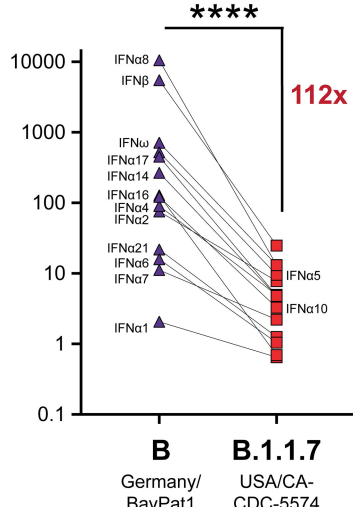
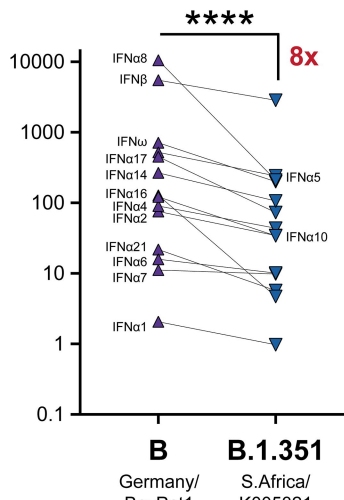
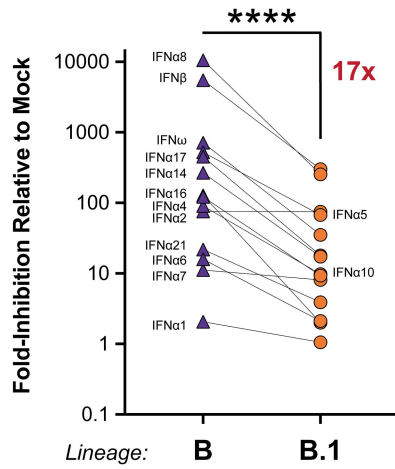
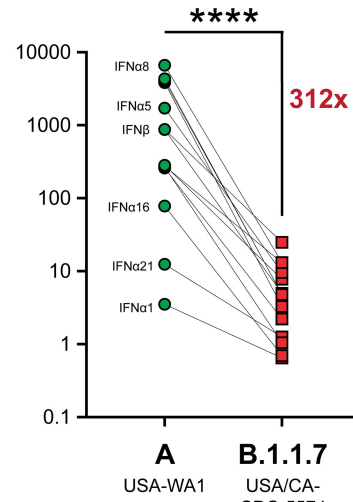
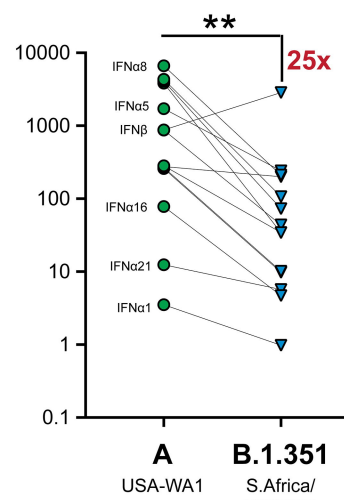
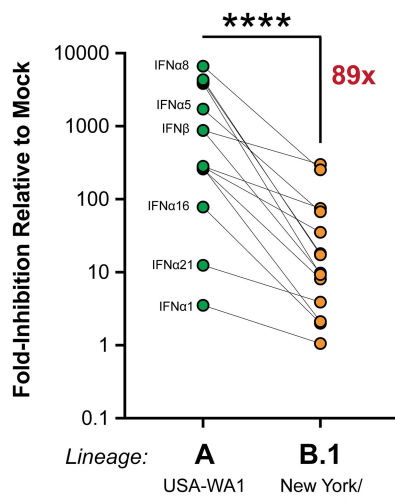
GISAID
Clade
Legend:

O	V	GV	GH+RBDx	GRY
S	G	GV+RBDx	GR	GRY+RBDx
L	G+RBDx	GH	GR+RBDx	

RBDx: relevant changes near receptor and antibody binding sites

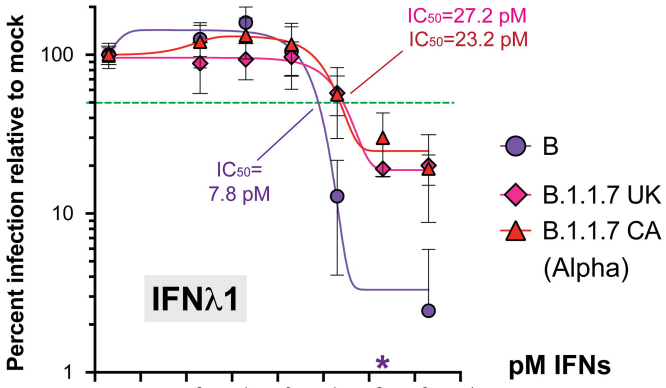
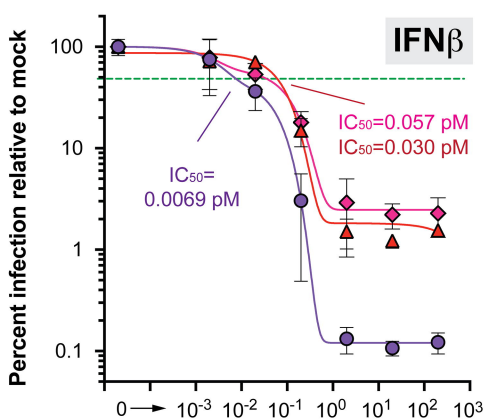
A**Screen for Potent IFNs****C****Potency of Diverse IFNs****B****Sensitivity of D614G SARS-CoV-2 variants to diverse Interferons****S.Africa/K005321/2020 Lineage B.1.351****New York-PV08410/2020 Lineage B.1****USA/CA_CDC_5574/2020 Lineage B.1.1.7**

A**IFN α subtypes: relationship between IFNAR signaling and SARS-CoV-2 inhibition****B****IFN α subtypes: relationship between IFNAR2 binding affinity and SARS-CoV-2 inhibition****C****IFN α subtypes: relationship between inhibition of HIV-1 and SARS-CoV-2**

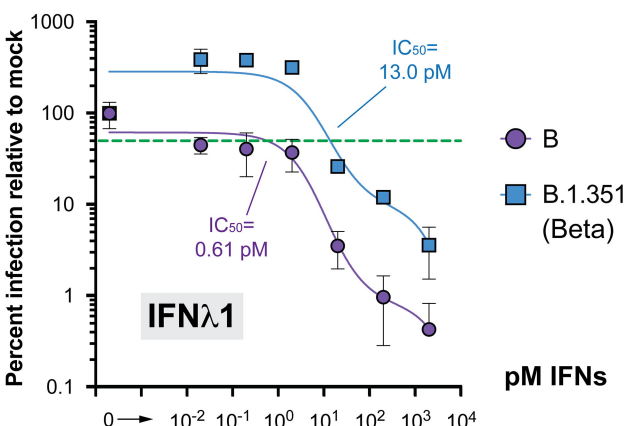
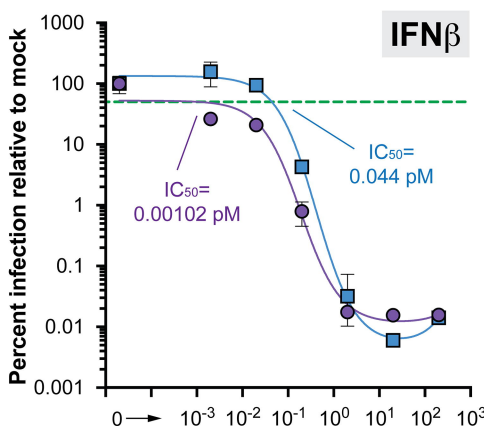
A**Heatmap: Fold-inhibition relative to mock****B****IFN-I resistance: A vs B****C****IFN-I resistance of SARS-CoV-2 variants (relative to lineage B)****D****IFN-I resistance of SARS-CoV-2 variants (relative to lineage A)**

Dose-titration of IFN β and IFN λ 1

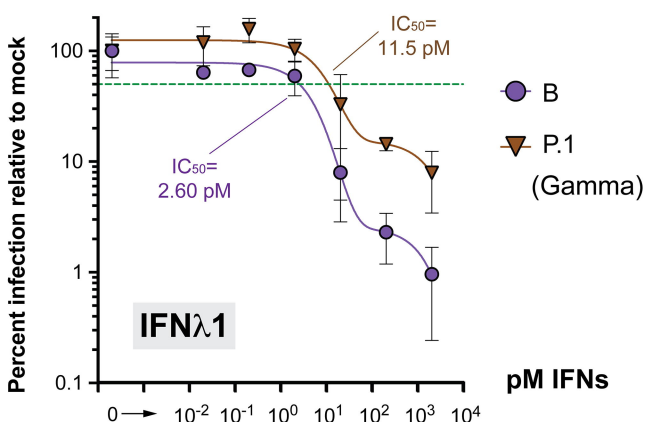
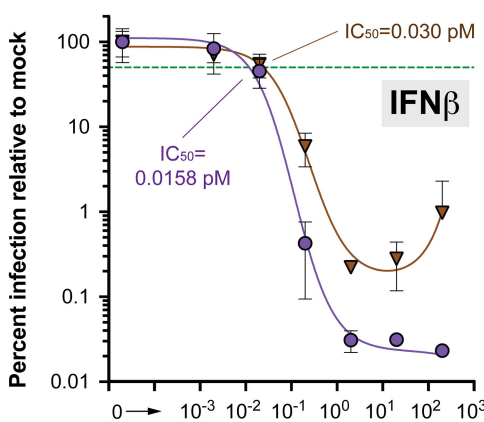
A



B



C



D

